Clean Energy Science and Technology 2024, 2(2), 169.
https://doi.org/10.18686/cest.v2i2.169

Article

Research on screening strategy of Organic Rankine Cycle working fluids based on quantum chemistry

Yi Wang, Jiawen Yang, Li Xia, Xiaoyan Sun, Shuguang Xiang, Lili Wang*

College of Chemical Engineering, Qingdao University of Science and Technology, Qingdao 266042, Shandong Province, People's Republic of China

*** Corresponding author:** Lili Wang, liliw@qust.edu.cn

CITATION

Wang Y, Yang J, Xia L, et al. Research on screening strategy of Organic Rankine Cycle working fluids based on quantum chemistry. Clean Energy Science and Technology. 2024; 2(2): 169. https://doi.org/10.18686/cest.v2i2.169

ARTICLE INFO

Received: 5 January 2024
Accepted: 6 April 2024
Available online: 14 May 2024

Abstract: The screening of working fluids is one of the key components in the study of power generation systems utilizing low-temperature waste heat. However, the variety of working fluids and their complex composition increase the difficulty of screening working fluids. In this study, a screening strategy for working fluids was developed from the perspective of the thermodynamic physical properties of working fluids. A comparative ideal gas heat capacity via the reduced ideal gas heat capacity factor (RCF) was proposed to characterize the dry and wet properties of working fluids, where RCF > 1 indicated a dry working fluid and RCF < 1 indicated a wet working fluid. A three-step screening strategy was developed for working fluid screening for organic Rankine cycles (ORCs). The strategy comprised basic physical property analysis of working fluids, research on dry and wet properties, and quantum chemical analysis. By comparing the RCF calculation result of 23 selected working fluid with values from the literature, the relative deviations of the data were less than 6.64% overall, indicating that the calculation result of the RCFs is reliable. The selection strategy explains the mechanism of working fluid selection in ORC systems from both micro- and macro-perspectives, laying a foundation for the study of structure-activity relationships in working fluids for ORCs.

Keywords: Organic Rankine cycle; selection of working fluids; RCF; thermodynamics

1. Introduction

China has become the world's largest energy producer and energy consumer, of which the industrial sector accounts for about 65% of the country's overall energy consumption, which is one of the main areas of energy saving and carbon reduction. A large amount of waste heat is generated during industrial operation, of which low-temperature waste heat (below 300 ℃) accounts for the highest proportion. The low temperature and recovery difficulty of low-temperature waste heat cause serious energy waste. Power generation using low-temperature waste heat is one of the important ways of waste heat recovery, which has significant economic and social benefits [1,2], and organic Rankine cycles (ORCs) have been widely used in realizing power generation using low-temperature waste heat.

The key to improving the efficient conversion of power generation cycle systems using low-temperature waste heat lies in the selection of efficient and environmentally friendly working fluids. The use of appropriate working fluids can improve waste heat conversion efficiency, save energy, and reduce consumption, which is in line with China's national policy of high-quality green development of the chemical industry. With the continuous deepening of research, based on the concept of low-carbon environmental protection and in accordance with the Kigali Amendment to the Montreal Protocol, the application of working fluids, such as hydrofluorocarbons

(HFCs), hydrochlorofluorocarbons (HCFCs), and chlorofluorocarbons (CFCs), has been phased down [3]. The screening of ORC working fluids mainly considers various factors, such as basic physical properties, safety, thermal stability, and environmental adaptability [4]. In addition, the safety and environmental performances, toxicity, flammability index, etc., of working fluids must also be taken into consideration [5,6]. Furthermore, ozone depletion potential (ODP) and global warming potential (GWP) are also two important indicators for working fluid screening. In addition, many studies have distinguished dry and wet types of working fluids through the difference in the slopes of the saturation curve in the thermoentropy diagram [7,8]. For wet working fluids, the saturation curve has a negative slope, which means that saturated steam easily produces a vapor-liquid mixture during the expansion process. For dry working fluids, the saturation curve has a positive slope, and the working fluid generates superheated steam during the expansion process [9,10]. Working fluids with nearly vertical saturation curves are called isentropic working fluids. In addition, some studies in the literature also reported other selection criteria for working fluids, such as low molecular entropy for better ORC thermal efficiency of working fluids [11,12]. There is a certain relationship between other thermodynamic properties of working fluids, such as critical temperature, evaporation enthalpy, molecular weight, compression factor, ideal gas isobaric heat capacity, ORC turbine work, ORC thermal efficiency, optimal heat source temperature, etc. [13–15]. Research works mainly conducted working fluid screening through the comparison of working fluid properties, working fluid structural properties, and ORC efficiency at the macro-scale. Since there are many types of working fluids, with working fluids having complex component structures, this increases the difficulty of working fluid screening, and the accuracy and speed of working fluid screening cannot be guaranteed.

With the advent of the Industry 4.0 era and the continuous development of quantum chemistry technology and molecular simulation technology, the innovative integration of digitalization, big data, and microstructure mechanism analysis methods has gradually become a research hotspot. Ingman et al. [16] used quantum chemical calculations to study molecular systems with complex structures to reduce costs. However, the density functional theory (DFT) of quantum chemistry has a low calculation accuracy for small molecules, which limits its application in small-molecule calculations. Bogojeski et al. [17] improved the accuracy of quantum chemical calculations by using machine learning to calculate the DFT density coupling cluster energy. Needham and Westmoreland [18] used quantum chemistry to calculate the kinetic parameters and thermochemical properties of refrigerant HFO-1234yf, analyze the potential single-molecule and bi-molecule destruction pathways of HFO-1234yf molecules, and provide theoretical support for the study of the chemical stability of the working fluid.

On the basis of the above research studies, this paper presents research on the screening method of working fluids for ORCs to reveal the micro-mechanism of working fluid screening from the microscopic scale by combining quantum chemistry and working fluid screening, which can provide important theoretical support and direction guidance for the intelligent screening of working fluids.

2. Calculation method

2.1. Thermodynamic calculation

Previous studies have shown that working fluids can be divided into three categories based on the trend in the slope of the temperature-entropy curve, namely dry working fluids, isentropic working fluids, and wet working fluids. The T-S curves of different working fluids are shown in **Figure 1**. It can be seen from the figure that when the saturation curve shows a positive slope in the temperature-entropy coordinate, that is, when the slope of the T-S curve (dT/dS) is greater than 0, the working fluid is a dry working fluid. When the slope of the T-S curve is less than 0, it is a wet working fluid, where the saturated steam will produce a vapor-liquid mixture during the expansion process. When the working fluid has an almost vertical saturation curve, that is, the slope of the T-S curve is equal to 0, it is an isentropic working fluid. Studies have shown that dry working fluids or isentropic working fluids are more suitable for ORC systems.

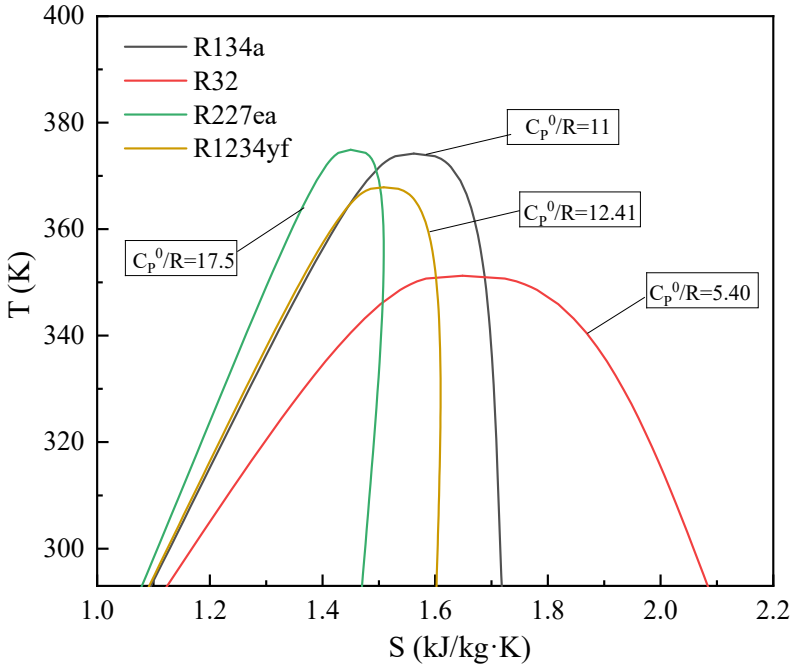

Figure 1. Different types of temperature entropy curves of working fluids.

The differences in the behaviors of dry, wet, and isentropic working fluids are mainly related to their molecular complexity. To accurately quantify the dry and wet characteristics of working fluids, it is necessary to first understand the calculation model related to it. The dry and wet characteristics of working fluids are related to entropy, and the calculation can be obtained through the thermodynamic relationship of entropy [19]. The formula is as follows:

$$dS = \frac{C_P}{T} dT - \left(\frac{\partial V}{\partial T}\right)_P dP \tag{1}$$

Assuming that entropy ΔS = 0 under reference states T_{ref} and P_{ref}, then:

$$S = -\int_{T_{ref},P_{ref}}^{T_{ref},P_H} \left(\frac{\partial V}{\partial T}\right)_P dP + \int_{T_{ref},P_H}^{T_H,P_H} \frac{C_P}{T} dT + \frac{\Delta H_H}{T_H} \tag{2}$$

$$\frac{dS}{dT_H} \approx \frac{C_P}{T_H} + 2\frac{d(\Delta H_H)}{d(T_H^2)} - \frac{\Delta H_H}{T_H^2} \tag{3}$$

where ΔH_H, T_H, and P_H are the evaporation enthalpy, evaporation temperature, and evaporation pressure, respectively [20]. According to Watson's equation [21], $\Delta H_{Hi} = \Delta H_{Hii}\left(\frac{1-T_{rHi}}{1-T_{rHii}}\right)^n$, where $T_{rHi} = \frac{T_{Hi}}{T_C}$ and $T_{rHii} = \frac{T_{Hii}}{T_C}$ denote the comparative evaporation temperatures, while ΔH_{Hi} and ΔH_{Hii} correspond to evaporation enthalpies of State i and State ii, respectively. Hence, for $\xi = \frac{ds}{dT_H}$, then:

$$\xi = \frac{C_P}{T_H} - \frac{\frac{n \cdot T_{rH}}{1-T_{rH}} + 1}{T_H^2}\Delta H_H \tag{4}$$

where n is a constant, typically 0.375 or 0.38.

This criterion is consistent with the trends of the slope of temperature-entropy of working fluids described above, that is, $\xi > 0$ for a dry working fluid, $\xi < 0$ for a wet working fluid, and $\xi = 0$ for an isentropic working fluid. According to the above thermodynamic relation of entropy, assuming that the working fluid is an ideal gas without a phase change, then:

$$dS = \frac{C_P}{T} dT \tag{5}$$

$$\frac{C_P^{ig}}{T} = \left(\frac{\partial S}{\partial T}\right)_P \tag{6}$$

$$\frac{C_P^{ig}}{R} = \frac{T}{R}\left(\frac{\partial S}{\partial T}\right)_P \tag{7}$$

The T in the formula refers to the average between the heat sink temperature, which is taken as 20 ℃, and the critical temperature of the mass.

Due to differences in the comparative specific heat capacity of working fluids, working fluid R134a was selected as the benchmark working fluid in this study, and the reduced ideal gas heat capacity factor (RCF) was defined to quantify its dry and wet characteristics.

$$RCF = \frac{\left(\frac{C_P^{ig}}{R}\right)_{wf}}{\left(\frac{C_P^{ig}}{R}\right)_{ref}} \tag{8}$$

where wf refers to the working fluid used in the actual ORC system and ref refers to reference working fluid R134a. Through calculations, since $(\frac{C_P^{ig}}{R})_{R134a} = 11$, then:

$$RCF = \frac{\left(\frac{C_P^{ig}}{R}\right)_{wf}}{11} \tag{9}$$

When $RCF > 1$, the working fluid is a dry working fluid, and when $RCF < 1$, it is a wet working fluid, while when $RCF = 0$, it is an isentropic working fluid. For a

working fluid, its comparative specific heat capacity is simple to obtain and highly accurate. This judgment method can be used to judge its dry and wet characteristics more efficiently.

Currently, the NIST database contains the ideal gas heat capacities of most working fluids, and the Joback group contribution method has been used to estimate for working fluids that lack data [21]. The calculation formula is as follows:

$$C_p^0 = \left[\sum_k N_k C_{pAk}^0 - 37.93\right] + \left[\sum_k N_k C_{pBk}^0 + 0.21\right] T + \left[\sum_k N_k C_{pCk}^0 - 0.000391\right] T^2 + \left[\sum_k N_k C_{pDk}^0 - 2.06 \times 10^{-7}\right] T^3 \quad (10)$$

where N is the number of k groups, and C_{pAk}^0, C_{pBk}^0, C_{pCk}^0, and C_{pDk}^0 are the contribution values of the k-th atom or group.

2.2. Quantum chemical calculation

Quantum chemistry is a method used to explain chemical problems based on quantum mechanics. It can be used to estimate the relative stability of molecules, calculate the properties of reaction intermediates, analyze and predict thermodynamic properties, etc. [22,23]. In this study, surface charge distribution and weak interaction analyses were used to analyze working fluids, and the mechanism of working fluid screening was discussed from a microscopic perspective. Surface charge distribution (σ-profile) refers to the probability determined by the cross section of charge density σ, which can be divided into hydrogen bond (HB) σ-profile and non-hydrogen bond σ-profile, which can be calculated with the following formula [24]:

$$p_i(\sigma) = \frac{n_i(\sigma)}{n_i} = \frac{A_i(\sigma)}{A_i} \quad (11)$$

$$n_i = \frac{A_i}{a_{eff}} \quad (12)$$

$$A_i = a_{eff} \sum_\sigma n_i(\sigma) \quad (13)$$

$$p_i^{nHB}(\sigma) = \frac{n_i^{nHB}(\sigma)}{n_i} = \frac{A_i^{nHB}(\sigma)}{A_i} \quad (14)$$

$$p_i^{HB}(\sigma) = \frac{n_i^{HB}(\sigma)}{n_i} = \frac{A_i^{HB}(\sigma)}{A_i} \quad (15)$$

where $A_i(\sigma)$ refers to the area of the molecular surface, $n_i(\sigma)$ is the number of molecular fragments with the surface area of $A_i(\sigma)$ and charge density of σ, and n_i is the number of single molecular fragments with a total surface area of A_i, while a_{eff} is the surface area of the standard line segment, and nHB and HB represent non-hydrogen bonding and hydrogen bonding, respectively [25].

The analysis of weak interactions of molecules is inseparable from physical properties. It often refers to various forms of interactions in which the intensity of intermolecular interactions is significantly weaker than that of general chemical bonds,

such as van der Waals interaction, π-π stacking, hydrogen bond, halogen bond, dihydrogen bond, etc. [26]. Visual analysis can be performed through the independent gradient model (IGM) and reduced density gradient (RDG) for intuitively understanding the weak interaction region and strength in molecules [27,28].

For the IGM, the area of interatomic interaction can be explicitly represented by function δg, which is divided into intra-fragment $\delta g_{\_intra}$ and inter-fragment $\delta g_{\_inter}$ interactions, calculated using the following equation:

$$g(r) = \left|\sum_i \nabla\rho_i(r)\right| g^{IGM}(r) = \left|\sum_i abs[\nabla\rho_i(r)]\right| \tag{16}$$

$$\delta g(r) = g^{IGM}(r) - g(r) \tag{17}$$

where i refers to the atomic number, $\nabla\rho$ is the gradient vector, $(\nabla\rho)$ is the absolute value of $\nabla\rho$, and $\|$ is the vector module.

RDG analysis uses the RDG isosurface to display the weak interaction region and projects the sign of the ρ function (lambda2) in different colors to display the weak interaction region. The average value of the RDG function can be calculated using the following formula [26,28]:

$$\overline{RDG(r)} = \frac{1}{2(3\pi^2)^{\frac{1}{3}}} \frac{\overline{|\nabla\rho(r)|}}{\overline{\rho(r)}^{\frac{4}{3}}} \tag{18}$$

where $\rho(r)$ and $\nabla\rho(r)$ refer to the average density and average density gradient, respectively.

3. Working fluid screening strategy

The selection of working fluids is a key component of ORC system research. Previous research works focused more on the efficiency of working fluids in ORC systems but ignored the close relationship between the physical properties of working fluids and ORC efficiency. The uncertainty of the working fluid screening mechanism directly affects the screening results of working fluids. The determination of a pre-screening strategy based on the physical properties of working fluids can effectively break through this bottleneck. In this study, a preliminary screening strategy for working fluids coupled with thermodynamics and quantum chemistry is proposed. The preliminary screening of working fluids is shown in **Figure 2**. As can be seen from the figure, the preliminary strategy for screening working fluids mainly comprised the following steps:

1) Preliminary selection based on basic properties: The REFPROP10.0 database and literature search for potential working fluids that can be used in ORC systems were combined to determine the basic thermodynamic properties and environmental characteristics (such as GWP, ODP, etc.) of working fluids. The initial screening of working fluids was carried out based on the temperature threshold of low-temperature waste heat (based on the evaporation temperature range of 100–180 ℃).
2) Judgment of dry and wet characteristics of working fluids: The T-S data of working fluids based on ΔS = 0 were determined and a T-S diagram was drawn. The comparative specific heat capacity factors (RCFs) of the working fluids were calculated to determine the type of working fluids (dry, isentropic, or wet).

3) Analysis based on quantum chemistry: Quantum chemical methods were used to calculate the surface charge distribution (σ-profile), determine the HB strength, and analyze the weak interactions of the working fluids. From the perspective of quantum chemistry, RDG and IGM were used in this study to verify the working fluid screening result.

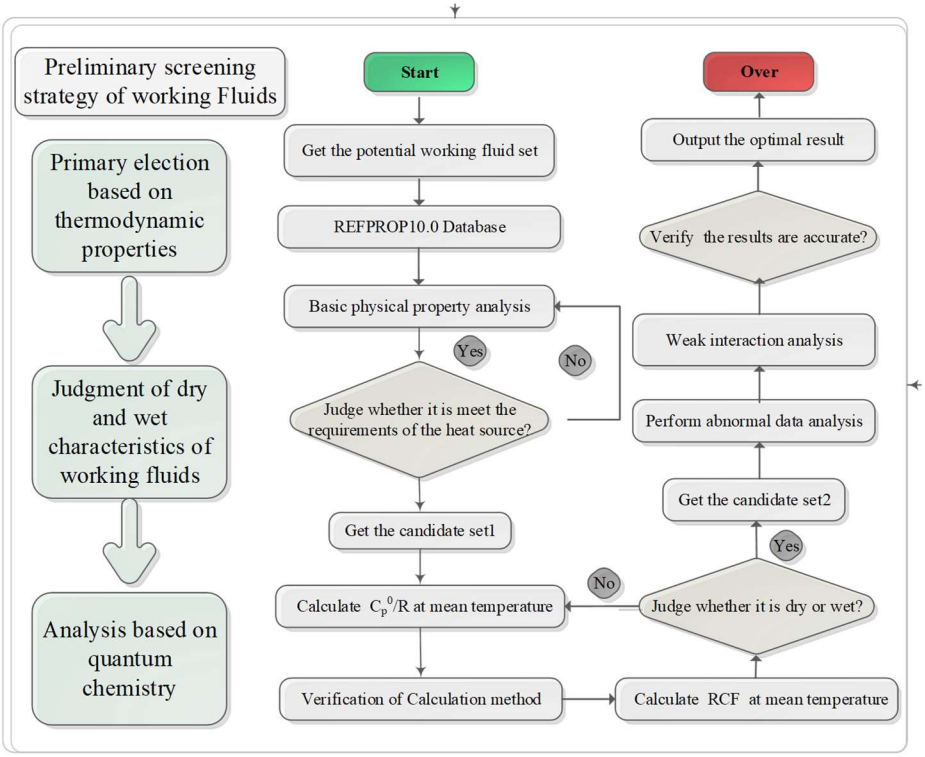

Figure 2. Block diagram of strategy for initial screening of working fluids.

4. Results and discussion

4.1. Verification of accuracy of calculation results

Process simulation software Aspen Plus was used to calculate the comparative specific heat capacities of different working fluids at average temperatures. Average temperature refers to the average between the critical temperature of a working fluid and the heatsink temperature (the heatsink temperature referenced from the literature is 20 ℃). The heat capacity factors of working fluids that do not exist in the database were estimated and determined by using GCMs. In order to verify the accuracy of the calculation result, the comparative specific heat capacity factors of 23 different types of working fluids were calculated and compared with values from the literature. The comparison result is shown in **Table 1**. The result showed that the relative deviations between the calculated data of 23 working fluids and the literature-obtained data were not high, and the absolute values of relative deviation were in the range of 0.05%–6.64%. Among them, the working fluid with the largest relative deviation was R347mcc (−6.64%). Although the calculated deviation of the comparative specific heat capacity of R347mcc was large, it did not affect the judgment of its working fluid type. This shows that the comparative specific heat capacity data obtained by this calculation method is reliable. According to the RCFs of the working fluids, their types

can be judged, which were found consistent with the types given in the literature. However, in this judgment method, since R125 belongs to the same HFC type as the benchmark working fluid and the RCF calculation results were similar, its RCF was at the boundary of the judgment benchmark, causing the judgment result to be invalid [11,29].

Table 1. Comparison of calculated data and literature-obtained data of comparative specific heat capacities of different working fluids [30,31].

Working fluid	Chemical name	C_p^0/R		Relative deviation (%)	RCF	Type of working fluid [30,31]
		Calculated value	Reference value			
R125	Pentafluoro ethane	11.76	11.80	−0.37	1.07	Wet
R218	Octafluoropropane	18.09	18.50	−2.24	1.68	Dry
R143a	Trifluoroethane	9.85	9.80	0.55	0.89	Wet
R32	Difluoromethane	5.38	5.40	−0.35	0.49	Wet
R290	Propane	9.61	9.60	0.08	0.87	Wet
R134a	Tetrafluoro ethane	11.02	11.00	0.19	1.00	Isentropic
R227ea	Heptafluoropropane	17.58	17.50	0.43	1.59	Dry
R152a	Difluoroethane	8.84	8.90	−0.73	0.81	Wet
R270	Cyclopropane	7.89	7.90	−0.12	0.72	Wet
R600a	Isobutane	13.29	13.40	−0.86	1.22	Dry
R142b	Chlorodifluoroethane	11.07	11.10	−0.26	1.01	Isentropic
R236ea	1,1,1,2,3,3-hexafluoropropane	16.74	17.00	−1.55	1.55	Dry
R245ca	1,1,2,2,3-pentafluoropropane	16.69	16.70	−0.05	1.52	Dry
R22	Difluoro chloromethane	6.91	6.80	1.57	0.62	Wet
R113	1,1,2-trifluoro-3-chloropropane	15.26	14.60	4.50	1.33	Dry
MM	Hexamethyldisilane	28.61	28.60	0.05	2.60	Dry
R115	Chloropentafluoroethane	13.01	13.20	−1.46	1.20	Dry
RC318	Octafluorocyclobutane	18.80	18.80	−0.01	1.71	Dry
R124-S	1,1,1,2-tetrafluoro-2-chloroethane	11.91	11.90	0.11	1.08	Isentropic
Dimethyl ether	Dimethyl ether	7.92	7.90	0.28	0.72	Wet
R347mcc	1-methoxyheptafluoropropane	19.88	21.30	−6.65	1.94	Dry
R123	Dichlorotrifluoroethane	12.32	12.30	0.17	1.12	Dry
R601a	Isopentane	14.27	14.30	−0.20	1.30	Dry

4.2. Working fluid screening based on basic properties

Based on the REFROP working fluid database and literature search, a total of 115 working fluids that can be used in an ORC system were collected. The working fluids were classified according to the working fluid classification, and the result is shown in **Figure 3**. From the figure, it can be seen that there were 6 kinds of CFC-type working fluids, 36 kinds of HC-type working fluids, 7 kinds of HCFC-type working fluids, 7 kinds of PFC-type working fluids, 15 kinds of HFC-type working fluids, 4 kinds of HCFO-type working fluids, 13 kinds of HFO-type working fluids, and 27 other types. Although the working fluids can meet the requirements of an ORC system, they are restricted by the temperature of the heat source. The temperatures of the low-temperature waste heat sources studied were in the range of 110–190 ℃, and the corresponding evaporation temperatures were 100–180 ℃. According to this constraint, some high-boiling-point working fluids can be initially screened out. In order to see the boiling point distributions of the 115 working fluids more clearly, the boiling point distribution diagram was statistically drawn, as shown in **Figure 4**.

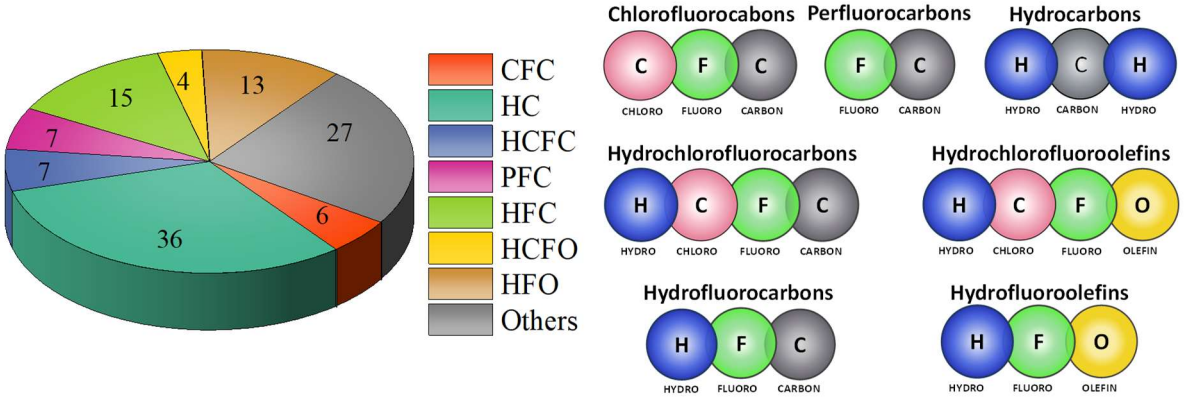

Figure 3. Classification of working fluids in the ORC system.

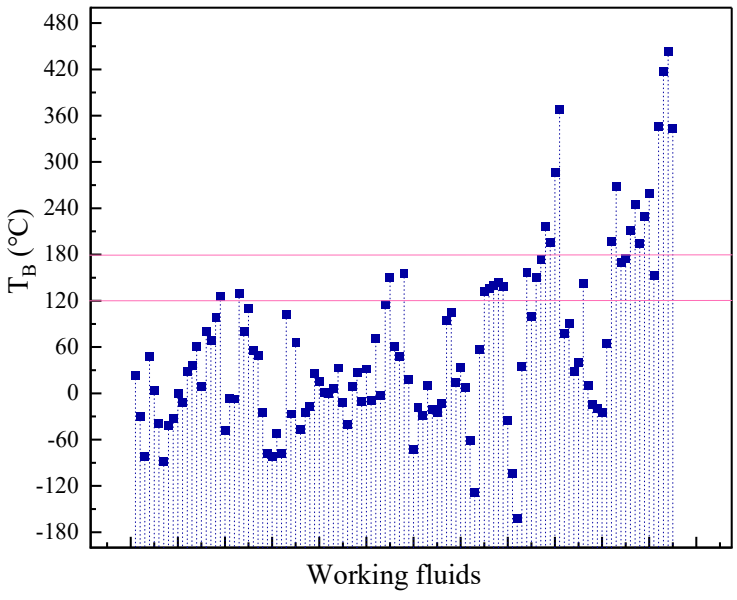

Figure 4. Boiling point distribution of 115 working fluids.

As shown in **Figure 4**, the boiling points of the working fluids were mostly distributed below 120 ℃. Considering the constraints of the temperature of low-temperature waste heat and the high toxicity of some working fluids (GWP > 8000, $T_{B,P=1atm}$ > 175 ℃, ODP ≥ 1), 30 working fluids with high boiling points were deleted. The distribution of the remaining 85 working fluids is shown in **Figure 5**. The working fluids were 6 CFCs, 22 HCs, 7 HCFCs, 7 PFCs, 15 HFCs, 4 HCFOs, 13 HFOs, and 11 other types.

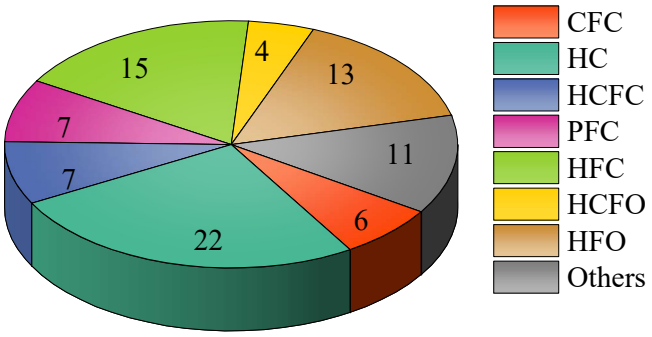

Figure 5. Classification of working fluids in the ORC system.

4.3. Judgment of characteristics of working fluids

The 85 working fluids screened according to the above steps were used to calculate their RCFs at average temperatures using process simulation software. For working fluids missing from the process simulation software database, their RCFs were estimated through customization and the Joback method. In addition, the RCFs of the different working fluids were calculated based on working fluid R134a. **Figure 6** shows that the data distribution of RCF fluctuations was within ±5%. It can be seen from the figure that the RCFs of most working fluids were greater than 1 and belonged to the dry working fluid type, while some data were close to 1 and belonged to the isentropic or wet working fluid type. The physical properties of some working fluids were estimated from the groups and may have calculation errors. Deletions were done by considering working fluids with smaller RCFs, such as R170, propadiene, R1150, R50, etc. A further analysis was required to determine the final deletion of working fluids. Among them, there were 11 groups of working fluids with RCFs less than 0.6, and 4 groups with RFCs between 0.6–0.75. Considering that wet working fluids are not suitable for ORC systems, working fluids with an RCF less than 0.75 were deleted. The classification of the working fluids after deletion is shown in **Figure 7**. It can be seen from the figure that the remaining 70 working fluids were 5 types of CFCs, 18 types of HCs, 7 types of HCFCs, 6 types of PFCs, 12 types of HFCs, 2 types of HCFOs, 12 types of HFOs (including working fluid R1216), and 6 other types.

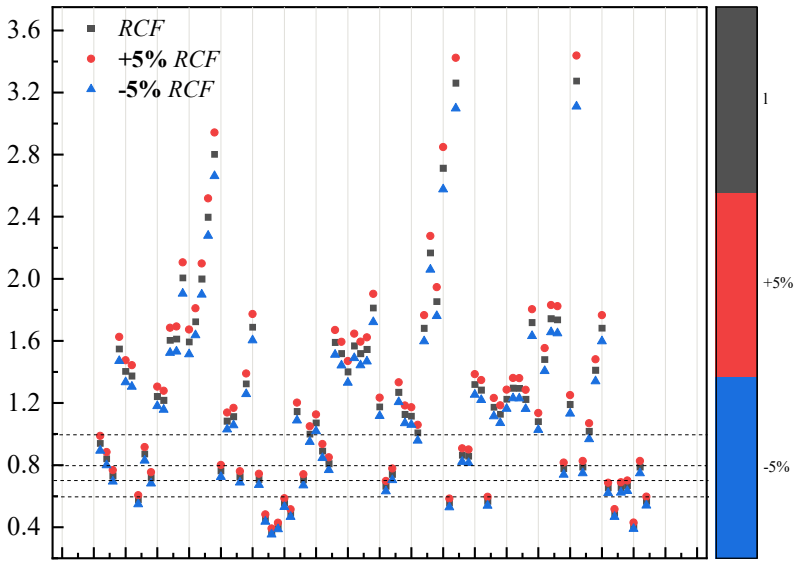

Figure 6. RCF distribution of 85 working fluids.

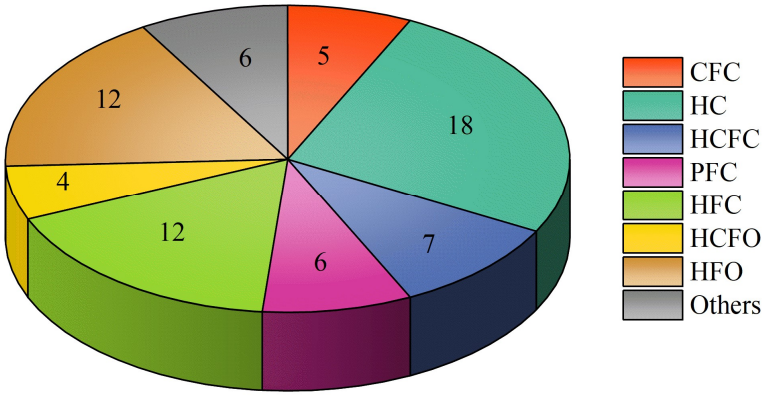

Figure 7. Classification of working fluids in ORC system.

4.4. Quantum chemical analysis

According to the above analysis results, 70 working fluids can be used in ORC systems and 15 working fluids were eliminated. These 15 working fluids are limited due to their dry and wet characteristics. The dry and wet characteristics of working fluids are related to their chemical structure [20]. Due to the strong hydrogen bonding between molecules, the vaporization enthalpy is relatively large. Therefore, working fluids with the hydrogen bonding interaction, such as water, ammonia, and alcohol, will produce large vaporization enthalpy and become wet working fluids. In order to better study the hydrogen bonding interaction of the deleted working fluid, the software Cosmos Logic and Gaussian 16W were used to analyze the impact of hydrogen bonding on the wet working fluid from the perspective of quantum chemistry [30]. The research was carried out through quantum chemical analysis, which comprised surface charge distribution analysis and weak interaction analysis.

The surface charge distribution curve was used to analyze whether these working fluids had hydrogen bonding capability, which was used to determine the relationship between the hydrogen bonding capability of the working fluids and their dry and wet characteristics. The surface charge distribution curves of 16 working fluids (reference

working fluid R134a and 15 eliminated working fluids) were calculated using Cosmos Logic, as shown in **Figure 8**. As can be seen from the figure, the surface charge distribution curve was divided into three parts: region $\sigma < -0.0082$ e/Å^2 is the hydrogen bond donor (HBD) region, where peaks in the surface charge distribution curve that fell in the HBD region indicated that the working fluid can provide hydrogen bonding); region $\sigma > +0.0082$ e/Å^2 is the HB acceptor (HBA) region, where peaks in the HBA region indicated that the working fluid can act as an acceptor for hydrogen bonding); and the nonpolar region (middle part), which had no hydrogen bonding effect [31,32]. It can be seen from **Figure 8** that the surface charge distribution curves of the 16 working fluids all had a wide range, but due to the different regional distributions of the peaks, their intensities were also different. Taking reference working fluid R134a as an example, the surface charge distribution curve corresponding to R134a had a wide range and two peaks, of which two strong peaks were in the non-polar region and a weak peak appeared at −0.01 e/Å^2. This showed that R134a has a weak HBD ability. In contrast, the surface charge distribution curves of EO, MeOH, R23, DCM, and R32 had multiple peaks, where the strong peaks were distributed in the HBD or HBA region, indicating the strong HBD or HBA ability of these working fluids to act as a donor or acceptor of hydrogen bonding. R1141, VCM, and R40 showed a weak peak in the HBD region and multiple strong peaks in the non-polar region, indicating that they have both non-polar characteristics and a weak HBD capability.

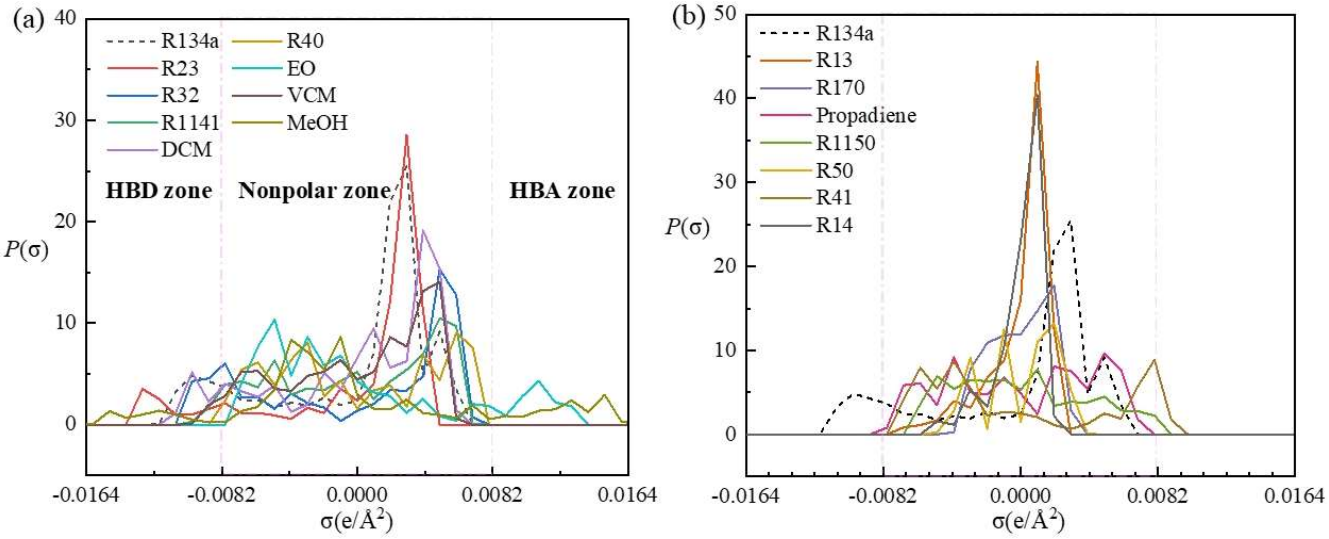

Figure 8. Surface charge distribution curves of 16 working fluids.

As can be seen from **Figure 8(b)**, the strong peak of the surface charge distribution curve of R41 was in the non-polar region, and a weak peak was in the HBA region, indicating that it has a weak HBA ability. The surface charge distribution curves of R1150 and allene had slight changes in HBA and HBD regions, and their strong peaks were all in the non-polar region, indicating that they have non-polar characteristics and may have weaker HBA and HBD capabilities. The surface charge distribution curves of other working fluids were all in the non-polar range, which proved that they have non-polar characteristics and do not have HBD and HBA

capabilities. The above analysis result showed that eight of the deleted working fluids have certain HBD and HBA capabilities, which means that hydrogen bonding can occur. These phenomena indicated that hydrogen bonding is one of the reasons rendering the wet property of working fluids.

While the other seven working fluids (propadiene, R1150, R13, R170, R50, R41, and R14) did not show HBD and HBA capabilities, this does not mean that they have no hydrogen bonding effect. Judging from the calculation mechanism of working fluids' surface charge density, the hydrogen bonding effect was determined based on the distribution area of the net potential on the molecular surface, which was not enough to express the hydrogen bonding interaction between working fluids' molecules. For this reason, the research also studied the hydrogen bonding interaction between the molecules of these seven working fluids.

Through quantum chemical calculations based on wave functions, RDG scatter plots (left side of **Figure 9**) and color isosurface plots (right side of **Figure 9**) of propadiene, R1150, R13, R170, R50, R41, and R14 were obtained. The colors of the corresponding areas of the left and right images were consistent. **Figure 9 (right)** depicts three color-filled isosurfaces, where green, blue, and red isosurfaces represented the presence of the van der Waals interaction, hydrogen bonding interaction, and steric effect, respectively. Thus, the van der Waals interaction, hydrogen-bonding interaction, and spatial effect corresponded to a green spike ($\lambda 2$) $\rho = 0.005$ a.u, a blue spike ($\lambda 2$) $\rho = -0.02$ a.u, and a red scattering ($\lambda 2$) $\rho = 0.010$ a.u, respectively, in the vicinity of the sign (**Figure 9 (left)**). As can be seen from the images on the right side of **Figure 9**, blue areas appear on the isosurface maps of the seven working fluids, indicating the existence of the HB interaction. There was almost no blue area in R50, indicating no HB effect. The spatial position of R13 did not show a red area, indicating that no spatial effect occurred. There were three blue isosurfaces with a darker color but a small area at the spatial positions of R134a and R41, indicating that the interaction strength was weak. This part of the interaction was provided by hydrogen and halogen bonds, and a small red area can be observed near the blue area due to steric effects. A small blue area appeared in the isosurfaces of R13 and R14, and the green area was larger, indicating that the van der Waals effect was stronger than the hydrogen bond (or halogen bond) effect. It can be seen from the RDG scatter plots that the blue scatter areas of R13 and R14 corresponded to the blue areas on the isosurfaces, which may be caused by hydrogen bonding due to the presence of halogen. The van der Waals effects of R13 and R14 corresponded to the green peaks near ($\lambda 2$) $\rho = -0.004$ a.u and 0.003 a.u in the RDG scatter plots, respectively. The isosurfaces of other working fluids, which were R170, R1150, R50, and propadiene, were mainly green. These working fluids are mainly comprised of small molecular alkanes and olefinic organic matter. The interaction between their molecules is mainly the van der Waals interaction, which is one of the reasons for the low boiling points of these working fluids. The above analysis result showed that weak interactions, such as hydrogen bonding and van der Waals interactions, are related to the wet property of working fluids.

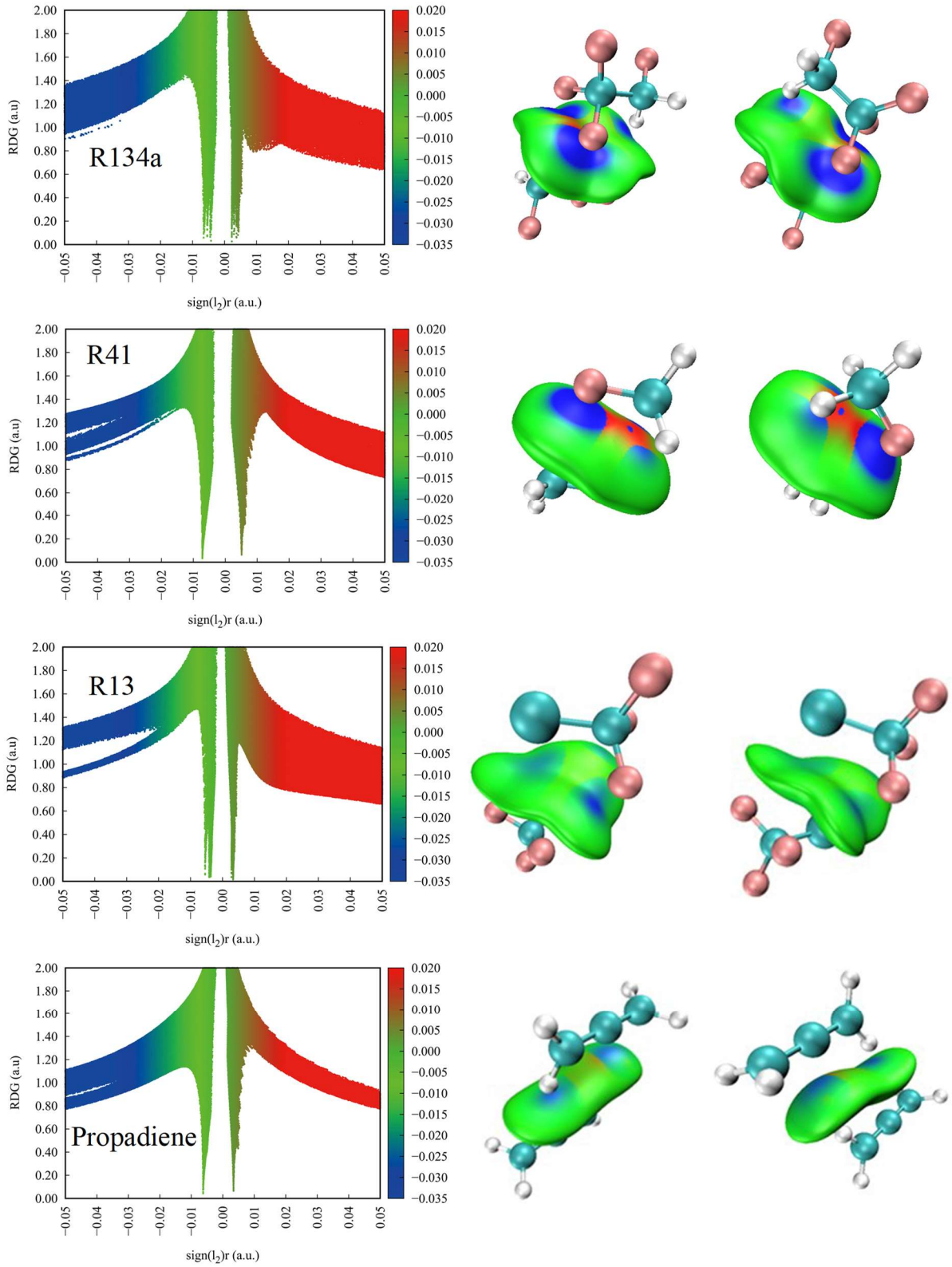

Figure 9. (*Continued*).

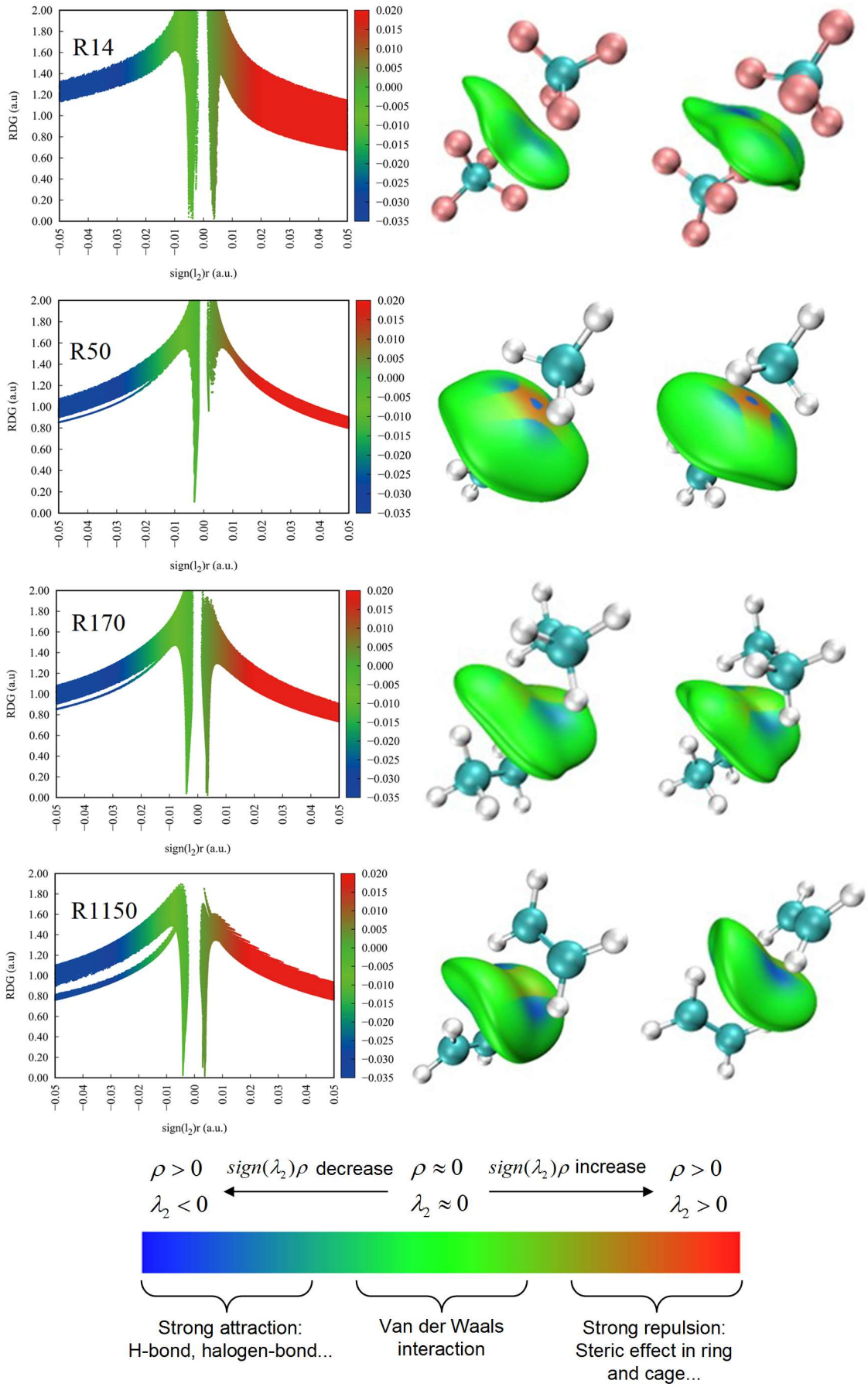

Figure 9. Surface charge distribution curves of 16 working fluids.

According to the above working fluid screening strategy, 70 working fluids suitable for ORCs were obtained. In order to verify the accuracy of the three-step method of the preliminary screening strategy, 10 candidate working fluids were selected using the preliminary screening strategy at an evaporation temperature of 180 °C, as shown in **Figure 10**. Toluene was finally determined as the most optimal working fluid through the three-step preliminary screening strategy, and the screening result is consistent with that from the literature [33]. Therefore, it can be shown that the working fluid obtained through the screening strategy can be well used in an ORC.

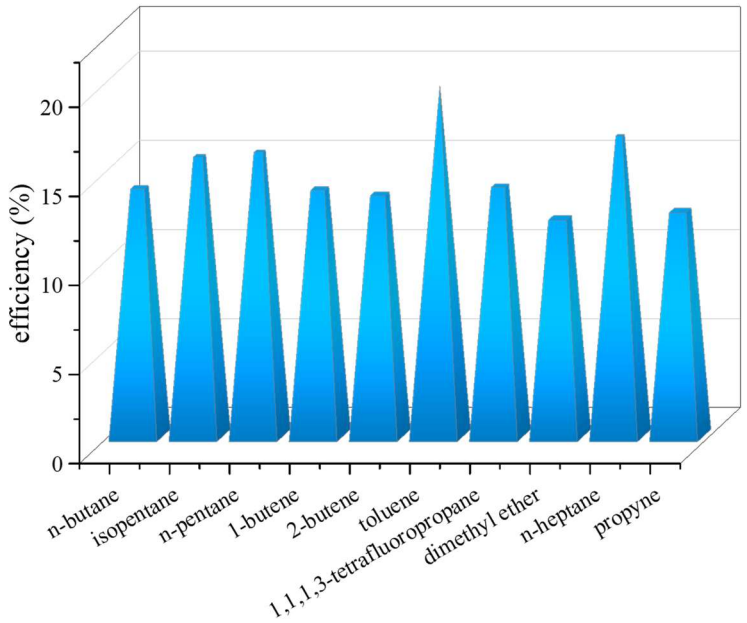

Figure 10. Application of three-step preliminary screening strategy [33].

Hence, through the above screening, 70 working fluids suitable for ORCs were obtained from 115 working fluids found in the existing literature. The working fluid screening result was verified through quantum chemical analysis. These working fluids can be used to carry out ORC application research in the future.

5. Conclusion

The ideal gas heat capacities of working fluids were determined by simulation and estimation, and comparative ideal gas heat capacity determination factors (RCFs), which characterize the dry and wet characteristics of working fluids, were derived through thermodynamic relations. Through a three-step method comprising basic physical property analysis of working fluids, research on dry and wet characteristics, and quantum chemical analysis, a preliminary screening strategy for working fluids suitable for ORC systems was determined. The main summary of the conclusion is as follows:

1) A calculation model for the thermodynamic properties and quantum chemical properties of working fluids was determined. An index was proposed for judging the dry and wet properties of working fluids, which was RCF, where a working

fluid is a dry working fluid when $RCF > 1$, a wet working fluid when $RCF < 1$, and an isentropic working fluid when $RCF = 1$.

2) A preliminary screening strategy for ORC systems' working fluids was determined. The strategy was divided into three main steps: screening based on basic properties, judgment of dry and wet properties of working fluids, and analysis based on quantum chemistry.
3) The accuracy of the calculation result was verified. The relative deviations between the calculated and literature-obtained RCF data of 23 selected working fluids were small. The absolute values of relative deviation were in the range of 0.05%–6.64%, and the maximum relative deviation was −6.64%. The result showed that the calculation result obtained by the above calculation method is reliable.
4) Through the above screening steps, 70 working fluids were finally determined for screening working fluids suitable for ORC systems. These working fluids included 5 CFCs, 18 HCs, 7 HCFCs, 6 PFCs, 12 HFCs, 2 HCFOs, 12 HFOs (including working fluid R1216), and 6 other working fluids. The effectiveness of the three-step preliminary screening strategy was verified through the case application.

Author contributions: Conceptualization, LX, LW and SX; methodology, XS and YW; software, JY; validation, YW, JY and LW; formal analysis, YW; investigation, JY; resources, YW, JY and LW; data curation, YW; writing—original draft preparation, YW; writing—review and editing, YW; visualization, JY; supervision, LW; project administration, LW; funding acquisition, SX. All authors have read and agreed to the published version of the manuscript.

Funding: We would like to thank the National Natural Science Foundation of China (No. 22178190) for providing financial support for this research project.

Conflict of interest: The authors declare no conflict of interest.

References

1. Sun R, Yang K, Wang B, et al. Technical and economic optimization of low-temperature waste heat recovery for supercritical carbon dioxide coal-fired power generation systems (Chinese). Thermal Power Generation. 2020; 010: 049.
2. Zhang C. Comprehensive Performance Evaluation and Experimental Study of Low-Grade Waste Heat Organic Rankine Cycle (Chinese) [PhD thesis]. Chongqing University; 2018.
3. Rowlands IH. The Fourth Meeting of the Parties to the Montreal Protocol: Report and Reflection. Environment: Science and Policy for Sustainable Development. 1993, 35(6): 25-34. doi: 10.1080/00139157.1993.9929109
4. Bao J, Zhao L. A review of working fluid and expander selections for organic Rankine cycle. Renewable and Sustainable Energy Reviews. 2013, 24: 325-342. doi: 10.1016/j.rser.2013.03.040
5. Martin TM, Young DM. Prediction of the Acute Toxicity (96-h LC50) of Organic Compounds to the Fathead Minnow (*Pimephales promelas*) Using a Group Contribution Method. Chemical Research in Toxicology. 2001, 14(10): 1378-1385. doi: 10.1021/tx0155045
6. Kondo S, Urano Y, Tokuhashi K, et al. Prediction of flammability of gases by using F-number analysis. Journal of Hazardous Materials. 2001, 82(2): 113-128. doi: 10.1016/s0304-3894(00)00358-7
7. Zhang X, Zhang Y, Wang J. New classification of dry and isentropic working fluids and a method used to determine their optimal or worst condensation temperature used in Organic Rankine Cycle. Energy. 2020, 201: 117722. doi: 10.1016/j.energy.2020.117722

8. Zhang T, Liu L, Hao J, et al. Correlation analysis based multi-parameter optimization of the organic Rankine cycle for medium- and high-temperature waste heat recovery. Applied Thermal Engineering. 2021, 188: 116626. doi: 10.1016/j.applthermaleng.2021.116626
9. Groniewsky A, Györke G, Imre AR. Description of wet-to-dry transition in model ORC working fluids. Applied Thermal Engineering. 2017, 125: 963-971. doi: 10.1016/j.applthermaleng.2017.07.074
10. Garrido JM, Quinteros-Lama H, Mejía A, et al. A rigorous approach for predicting the slope and curvature of the temperature–entropy saturation boundary of pure fluids. Energy. 2012, 45(1): 888-899. doi: 10.1016/j.energy.2012.06.073
11. Lukawski MZ, Tester JW, DiPippo R. Impact of molecular structure of working fluids on performance of organic Rankine cycles (ORCs). Sustainable Energy & Fuels. 2017, 1(5): 1098-1111. doi: 10.1039/c6se00064a
12. Wang J, Zhang J, Chen Z. Molecular Entropy, Thermal Efficiency, and Designing of Working Fluids for Organic Rankine Cycles. International Journal of Thermophysics. 2012, 33(6): 970-985. doi: 10.1007/s10765-012-1200-6
13. Stijepovic MZ, Linke P, Papadopoulos AI, et al. On the role of working fluid properties in Organic Rankine Cycle performance. Applied Thermal Engineering. 2012, 36: 406-413. doi: 10.1016/j.applthermaleng.2011.10.057
14. Palma-Flores O, Flores-Tlacuahuac A, Canseco-Melchorb G. Simultaneous molecular and process design for waste heat recovery. Energy. 2016, 99: 32-47. doi: 10.1016/j.energy.2016.01.024
15. Papadopoulos AI, Stijepovic M, Linke P. On the systematic design and selection of optimal working fluids for Organic Rankine Cycles. Applied Thermal Engineering. 2010, 30(6-7): 760-769. doi: 10.1016/j.applthermaleng.2009.12.006
16. Ingman VM, Schaefer AJ, Andreola LR, et al. QChASM: Quantum chemistry automation and structure manipulation. WIREs Computational Molecular Science. 2020, 11(4). doi: 10.1002/wcms.1510
17. Bogojeski M, Vogt-Maranto L, Tuckerman ME, et al. Quantum chemical accuracy from density functional approximations via machine learning. Nature Communications. 2020, 11(1). doi: 10.1038/s41467-020-19093-1
18. Needham CD, Westmoreland PR. Combustion and flammability chemistry for the refrigerant HFO-1234yf (2,3,3,3-tetrafluoropropene). Combustion and Flame. 2017, 184: 176-185. doi: 10.1016/j.combustflame.2017.06.004
19. Chen H, Goswami DY, Stefanakos EK. A review of thermodynamic cycles and working fluids for the conversion of low-grade heat. Renewable and Sustainable Energy Reviews. 2010, 14(9): 3059-3067. doi: 10.1016/j.rser.2010.07.006
20. Liu BT, Chien KH, Wang CC. Effect of working fluids on organic Rankine cycle for waste heat recovery. Energy. 2004, 29(8): 1207-1217. doi: 10.1016/j.energy.2004.01.004
21. Poling BE, Prausnitz JM, O'Connell JP. Properties of Gases and Liquids, 5th ed. McGraw-Hill Education; 2001.
22. Linderberg J, Öhrn Y, Brändas EJ, et al. Per-Olov Löwdin. Löwdin Volume. Published online 2017: 1-7. doi: 10.1016/bs.aiq.2016.04.001
23. Boeyens JCA. Quantum Chemistry. The Theories of Chemistry. Published online 2003: 261-332. doi: 10.1016/b978-044451491-2/50018-7
24. Tu W, Bai L, Zeng S, et al. An ionic fragments contribution-COSMO method to predict the surface charge density profiles of ionic liquids. Journal of Molecular Liquids. 2019, 282: 292-302. doi: 10.1016/j.molliq.2019.03.004
25. Grensemann H, Gmehling J. Performance of a Conductor-Like Screening Model for Real Solvents Model in Comparison to Classical Group Contribution Methods. Industrial & Engineering Chemistry Research. 2005, 44(5): 1610-1624. doi: 10.1021/ie049139z
26. Johnson ER, Keinan S, Mori-Sánchez P, et al. Revealing Noncovalent Interactions. Journal of the American Chemical Society. 2010, 132(18): 6498-6506. doi: 10.1021/ja100936w
27. Lu T, Chen F. Multiwfn: A multifunctional wavefunction analyzer. Journal of Computational Chemistry. 2011, 33(5): 580-592. doi: 10.1002/jcc.22885
28. Wu W, Yang Y, Wang B, et al. The effect of the degree of substitution on the solubility of cellulose acetoacetates in water: A molecular dynamics simulation and density functional theory study. Carbohydrate Research. 2020, 496: 108134. doi: 10.1016/j.carres.2020.108134
29. Lukawski MZ, DiPippo R, Tester JW. Molecular property methods for assessing efficiency of organic Rankine cycles. Energy. 2018, 142: 108-120. doi: 10.1016/j.energy.2017.09.140
30. Emamian S, Lu T, Kruse H, et al. Exploring Nature and Predicting Strength of Hydrogen Bonds: A Correlation Analysis Between Atoms-in-Molecules Descriptors, Binding Energies, and Energy Components of Symmetry-Adapted Perturbation Theory. Journal of Computational Chemistry. 2019, 40(32): 2868-2881. doi: 10.1002/jcc.26068

31. Li G, Gui C, Dai C, et al. Molecular Insights into SO2 Absorption by [EMIM][Cl]-Based Deep Eutectic Solvents. ACS Sustainable Chemistry & Engineering. 2021, 9(41): 13831-13841. doi: 10.1021/acssuschemeng.1c04639
32. Klamt A. COSMO-RS: From Quantum Chemistry to Fluid Phase Thermodynamics and Drug Design. Elsevier; 2005.
33. AL-Arfi I, Shboul B, Poggio D, et al. Thermo-economic and design analysis of a solar thermal power combined with anaerobic biogas for the air gap membrane distillation process. Energy Conversion and Management. 2022; 257: 115407. doi: 10.1016/j.enconman.2022.115407